Published in final edited form as:
Macromol Res. 2013 May 1; 21(5): 565–573. doi:10.1007/s13233-013-1050-5.

Synthesis and Biological Evaluation of Substrate-Based Imaging Agents for the Prostate-Specific Membrane Antigen

Youngjoo Byun[1,2], **Mrudula Pullambhatla**[1], **Haofan Wang**[1], **Ronnie C. Mease**[1], and **Martin G. Pomper**[*,1]

[1]Department of Radiology, School of Medicine, Johns Hopkins Medical Institutions, Baltimore, MD 21231, USA

[2]College of Pharmacy, Korea University, Chungnam 339-700, Korea

Abstract

Prostate-specific membrane antigen (PSMA) is an attractive target for the imaging of prostate cancer (PCa) due to the elevated expression on the surface of prostate tumor cells. Most PSMA-targeted low molecular weight imaging agents are inhibitors of PSMA. We have synthesized a series of substrate-based PSMA-targeted imaging agents by mimicking poly-γ-glutamyl folic acid, an endogenous substrate of PSMA. *In vitro* the γ-linked polyglutamate conjugates proved to be better substrates than the corresponding α-linked glutamates. However, *in vivo* imaging studies of γ-ray-emitting and γ-linked glutamates did not demonstrate selective uptake in PSMA-pos-itive over PSMA-negative tumors. Subsequent chromatographic studies and *in silico* molecular dynamics simulations indicated that hydrolysis of the substrates is slow and access to the enzymatic active site is limited. These results inform the design of future substrate-based imaging agents for PSMA.

Keywords

molecular imaging; prodrug; prostate cancer; SPECT; PSMA

Introduction

Prostate-specific membrane antigen (PSMA), a type II integral membrane metalloprotease, is an attractive target for imaging of prostate cancer (PCa) because it is highly expressed on the surface of prostate carcinomas, particularly those associated with castration-resistant and metastatic disease.[1] The extracellular active site of PSMA is readily accessed by a variety of chemical structures, many of which have been fashioned into imaging agents for a variety of modalities.[2–7]

PSMA is active as the dimer, each monomer of which is comprised of 750 amino acids. Two zinc ions are found at the active site of PSMA and are involved in the hydrolytic cleavage of endogenous substrates, including *N*-acetylaspartylglutamate (NAAG) in the brain and poly-

[*]Corresponding Author. mpomper@jhmi.edu.

γ-glutamyl folic acid in the intestine. Accordingly, PSMA has been referred to as glutamate carboxypeptidease II (GCPII) in the brain and folate hydrolase I (FOLH1) in the intestine. In the brain PSMA modulates the concentration of glutamate in the synaptic cleft through cleavage of NAAG. Abnormal concentrations of glutamate in the brain may be associated with a variety of disorders including ischemia, traumatic brain injury, amyotrophic lateral sclerosis, and schizophrenia.[8–12] FOLH1 hydrolyzes glutamates from the C-terminus of poly-γ-glutamyl folate to produce folic acid, a methyl donor in the synthesis of DNA.[13] PSMA is also found in the neovasculature of a variety of non-prostate solid tumors.[14] These diverse effects of PSMA render it an important target for the study of both central nervous system disease and cancer.[1,15]

Over the past decade, X-ray crystal structures of PSMA in complex with a variety of inhibitors or substrates have provided detailed information on the active site,[16,17] which has enabled rational ligand design. According to those crystal structures, the active site is composed of two distinct pockets, a so-called 'glutamate-sensing' pocket (S1') and the non-pharmacophore pocket (S1). The S1'pocket is highly sensitive to structural modification of putative ligands, having a nearly absolute requirement for a glutamate moiety, which make strong salt bridges with Arg 210 and Lys 699. Recent reports of P1'-modified inhibitors and substrates have demonstrated that the lipophilic alkyl chain of the P1'moiety also provides hydrophobic interactions with lipophilic amino acids in the S1'-site.[18,19] In the S1 pocket the side chains of amino acids are flexible and can undergo rearrangement upon interaction with various functional groups. In the absence of ligand, three arginines (Arg463, Arg534, and Arg536) are in a stacked conformation, which forms an additional subpocket, known as an "arginine patch," upon productive ligand binding.[20] In addition to the S1' and S1 sites, a flexible cylinder-like, 20 Å-deep tunnel exists adjacent to the S1 pocket and undergoes a conformational change upon ligand binding.[3,21] The tunnel region extends the hydrophilic surface area of the enzyme and can accommodate bulky and hydrophilic scaffolds. The tunnel region is much more flexible than the two aforementioned pockets and undergoes an inducedfit to accommodate the bulky linker of a variety of conjugates that bind to PSMA. We and others have used the tunnel region to develop inhibitor-based imaging agents conjugated with bulky functional groups, including radiometal-coordinating species and optical dyes.[5–7,21]

But apart from ligand-mediated internalization of PSMA,[22,23] which may regenerate the protein on the cell surface available for binding by another ligand, there is no amplification mechanism for concentration of targeted imaging agents within PSMA-expressing cells. Such amplification can increase the sensitivity of detection of those cells, as has been demonstrated for other enzyme- and transporter-based imaging agents.[24–26] The enzymatic activity of PSMA has been exploited for the targeted delivery of therapeutic agents. Mhaka and coworkers have targeted PSMA with toxic species by linking them to poly-γ-glutamates and poly-glutamate-asparates, with various permutations of aspartate and glutamate in α-or γ-linkages.[27] Anderson and coworkers reported a number of *N*-acyldipeptide-derived PSMA substrates to monitor PSMA activity by identifying the cleaved product by highperformance liquid chromatography (HPLC).[28]

In an effort to leverage the amplification possible with enzymatic turnover of suitably functionalized substrates, we describe the development of potential substrate-based imaging agents for PSMA. The agents designed mimic the endogenous substrate, poly-γ-glutamyl folate. We have designed α- or γ-linked glutamate conjugates linked to aminostrylpyridinium (ASP) dyes, on which ^{125}I and a lipophilic alkyl chain have been introduced (Figure 1). The ASP dye was intended to enable intercalation within the cell membrane of the radioactive species liberated upon cleavage.[29–31] Amphiphilic ASP dye was expected to orient with the polar head protruding from and the lipophilic tail embedded within, the cell membrane. It also provides the capacity to study cellular uptake with optical methods.[30,31] In order to modulate the hydrophilicity/lipophilicty of the substrates, we introduced penta- or hexa-glutamates. Our goal is to uncover a conjugate, the radiolabeled, cleaved product of which can be incorporated into the cell membrane with concurrent signal amplification *in vivo*. Here we focus on validating the concept of substrate-based imaging agents for PSMA and obtaining basic information on substrate properties for further structural modification.

Experimental

Materials

The protected amino acids and Fmoc-Glu(OtBu)-COOH preloaded Wang resin were purchased from ChemImpex (Chicago, IL). Chemicals and solvents for chemical reactions and for high-performance liquid chromatography (HPLC) were of reagent grade, were acquired from Sigma-Aldrich (Milwaukee, WI) or Fisher Scientific (Pittsburgh, PA), and were used without further purification. [^{125}I]NaI was purchased from MP Biomedicals (Costa Mesa, CA).

HPLC Analysis

The purity of final products was analyzed using a Waters (Milford, MA) HPLC apparatus using a NovaPak C18 reverse phase column (7.8 mm×300 mm, pore size: 6 μm). Separation of the products was achieved using an isocratic method of water (0.1% TFA) and acetonitrile or methanol (0.1% TFA). Reverse phase radio-HPLC purifications of ^{125}I-labeled compounds were performed using a Waters 510 pump, Waters 490E variable wavelength UV/vis detector at 254 nm and a Bioscan Flow Count PMT radioactivity detector (Washington, DC).

NMR and Mass Spectrometry

Mass spectra of positive ions were recorded with an ESI Bruker Esquire 3000 plus mass spectrometer (BrukerDaltonics, Billerica, MA) and ^{1}H NMR and ^{13}C NMR spectra were obtained on a Bruker Avance 400 MHz Spectrometer (Bruker Daltonics, Billerica, MA).

Chemistry

General Procedure for the Syntheses of 3a–3b (Scheme I)—The syntheses of **3a–3b** were accomplished from aniline by following published procedures.[32,33]

General Procedure for the Syntheses of 4a–4c (Scheme I)—To a solution of 3-bromo-4-methylpyridine (1 mmol) in anhydrous diethylether (4 mL) was added LDA (1.1 mmol, 0.55 mL, 2 M) at −78 °C. The suspension was stirred for 30 min at the same temperature. To the reaction mixture was added a solution of aldehyde **3a**–**3c** (1 mmol) in anhydrous THF (2 mL) at −78 °C. The reaction mixture stirred for additional 30 min at the same temperature and for 12 h at room temperature. Diethylether (50 mL) was added and the ether layer was washed with NH_4Cl solution (1 M, 25 mL×2). The organic layer was dried over Na_2SO_4, filtered, and evaporated. The residue was purified by silica gel column chro-matography (hexane:ethylacetate=3:2) to give **4a**–**4c** in 62%, 59%, and 66%, respectively.

2-(3-Bromopyridin-4-yl)-1-(4-(dihexylamino)phenyl)ethanol (4a)—^{1}H NMR ($CDCl_3$): 8.62 (s, 1H), 8.34 (d, 1H, J=4.9 Hz), 7.20 (d, 2H, J=8.7 Hz), 7.19 (d, 1H, J=4.9 Hz) 6.60 (d, 2H, J=8.7 Hz), 4.88–4.92 (m, 1H), 3.25 (t, 4H, J=7.8 Hz), 3.12–3.15 (m, 2H), 1.55–1.59 (m, 4H), 1.29–1.33 (m, 12H), 0.90 (t, 6H, J=6.6 Hz), ^{13}C NMR ($CDCl_3$): 151.5, 150.3, 147.6, 147.4, 131.4, 126.8, 126.7, 123.4, 112.4, 72.3, 44.9, 40.6, Theoretical MS $C_{25}H_{37}BrN_2O$: 460.21, observed: $[M+H]^+$; 461.2.

2-(3-Bromopyridin-4-yl)-1-(4-(didodecylamino)phenyl) ethanol (4b)—^{1}H NMR ($CDCl_3$): 8.66 (s, 1H), 8.36 (d, 1H, J=4.5 Hz), 7.23 (d, 2H, J=8.2 Hz), 7.21 (d, 1H, J=4.5 Hz) 6.61 (d, 2H, J=8.2 Hz), 4.89–4.93 (m, 1H), 3.26 (t, 4H, J=7.6 Hz), 3.11–3.14 (m, 2H), 1.54–1.58 (m, 4H), 1.27–1.33 (m, 36H), 0.89 (t, 6H, J=6.7 Hz), ^{13}C NMR ($CDCl_3$): 151.69, 148.04, 147.80, 147.36, 129.53, 126.87, 126.68, 123.47, 111.43, 72.62, 51.05, 44.65, 31.86, 29.65, 29.55, 29.52, 29.30, 27,15, 22.65, 14.10, Theoretical $MSC_{37}H_{61}BrN_2O$: 628.40, observed: $[M+H]^+$; 629.5.

2-(3-Bromopyridin-4-yl)-1-(4-(dimethylamino)phenyl) ethanol (4c)—^{1}H NMR ($CDCl_3$): 8.52 (s, 1H), 8.24 (d, 1H, J=4.5 Hz), 7.24 (d, 2H, J=8.2 Hz), 7.11 (d, 1H, J=4.5 Hz) 6.69 (d, 2H, J=8.2 Hz), 4.87–4.90 (m, 1H), 3.08–3.11 (m, 2H), 2.94 (s, 6H), ^{13}C NMR ($CDCl_3$): 151.5, 150.3, 147.6, 147.4, 131.4, 126.8, 126.7, 123.4, 112.4, 72.3, 44.9, 40.6, Theoretical $MSC_{15}H_{17}BrN_2O$: 320.05, observed: $[M+H]^+$; 320.8.

General Procedure for the Syntheses of 5a–5c (Scheme I)—To a solution of carbinol (0.5 mmol) in dioxane (10 mL) was added a 3 N-HCl solution (2 mL) at room temperature. The reaction mixture was stirred at 60 °C for 6 h. The progress of the reaction was monitored by thin layer chromatography (TLC). After removing the excess dioxane, $NaHCO_3$ solution (3 N, 2 mL) was added to adjust pH ~7. The aqueous layer was extracted with dichloromethane (50 mL). The organic layer was dried over Na_2SO_4, filtered, and evaporated. The residue was purified by silica gel column chromatography (hexane:ethylacetate=3:1, 0.1% triethylamine) to give aminostrylpyridines **5a–5c**, respectively.

(E)-4-(2-(3-Bromopyridin-4-yl)vinyl)-*N*,*N*-dihexylaniline (5a)—^{1}H NMR ($CDCl_3$): 8.65 (s, 1H), 8.37 (d, 1H, J=5.2 Hz), 7.48 (d, 1H, J=5.2 Hz), 7.44 (d, 2H, J=8.8 Hz) 7.24 (d, 1H, J=16.1 Hz), 7.15 (d, 1H, J=16.1 Hz), 6.62 (d, 2H, J=8.8 Hz), 3.30 (t, 4H, J=7.8 Hz),

1.56–1.60 (m, 4H), 1.31–1.35 (m, 12H), 0.91 (t, 6H, J=6.8 Hz), Theoretical $MSC_{25}H_{35}BrN_2$: 442.20, observed: $[M+H]^+$; 443.3.

(E)-4-(2-(3-Bromopyridin-4-yl)vinyl)-*N*,*N*-didodecyl-aniline (5b)—^{1}H NMR ($CDCl_3$): 8.65 (s, 1H), 8.38 (d, 1H, J=5.2 Hz), 7.49 (d, 1H, J=5.2 Hz), 7.44 (d, 2H, J=8.8 Hz), 7.20 (d, 1H, J=16.1 Hz) 7.10 (d, 1H, J=16.1 Hz), 6.62 (d, 2H, J=8.8 Hz), 3.30 (t, 4H, J=7.4 Hz), 1.57–1.61 (m, 4H), 1.27–1.32 (m, 36H), 0.88 (t, 6H, J=7.0 Hz), ^{13}C NMR ($CDCl_3$): 152.41, 148.86, 147.80, 144.99, 135.56, 128.93, 122.82, 121.17, 119.51, 118.71, 111.41, 51.02, 31.86, 29.62, 29.53, 29.49, 29.29, 27.24, 27.10, 22.65, 14.10, Theoretical $MSC_{37}H_{59}BrN_2$: 610.39, observed: $[M+H]^+$; 611.4.

(E)-4-(2-(3-Bromopyridin-4-yl)vinyl)-*N*,*N*-dimethyl-aniline (5c)—^{1}H NMR ($CDCl_3$): 8.66 (s, 1H), 8.39 (d, 1H), 7.46–7.50 (m, 3H), 7.22 (d, 1H) 7.13 (d, 1H), 6.71 (d, 2H), 3.02 (s, 6H), Theoretical $MSC_{15}H_{15}BrN_2$: 302.04, observed: $[M+H]^+$; 303.1.

General Procedure for the Syntheses of 6a–6c (Scheme I)—To a solution of substituted aminostrylpyridine (**5a–5c**, 1 mmol) in anhydrous DMF (10 mL) was added $Pd(OAc)_2$ (2.5 mol%), PPh_3 (5 mol%), TEA (5 mmol) and ethylacrylate (1.5 mmol) under nitrogen purge. The reaction mixture was stirred at 120 °C for 48 h. The mixture was cooled down and diluted with 10 mL of water. The aquous layer was extracted with ethylacetate (30 mL). The organic layer was washed with brine, dried over Na_2SO_4, and filtered through Celite. After evaporating the excess solvent, the residue was purified by silica gel column chromatography (hexane:ethylacetate=3:1) to give aminostrylpyridine acrylate (**6a–6c**).

(E)-Ethyl 3-(4-(4-(dihexylamino)styryl)pyridin-3-yl)acry-late (6a)—^{1}H NMR ($CDCl_3$): 8.67 (s, 1H), 8.45 (d, 1H, J=5.3 Hz), 8.04 (d, 1H, J=16.0 Hz), 7.44 (d, 1H, J=5.4 Hz) 7.41 (d, 2H, J=8.8 Hz), 7.14 (d, 1H, J=16.0 Hz), 7.02 (d, 1H, J=16.0 Hz), 6.61 (d, 2H, J=8.8 Hz), 6.41 (d, 1H, J=16.0 Hz), 4.29 (q, 2H, J=J=7.1 Hz), 3.30 (t, 4H, J=7.8 Hz), 1.56–1.60 (m, 4H), 1.31–1.37 (m, 15H), 0.90 (t, 6H, J=6.7 Hz), ^{13}C-NMR ($CDCl_3$): 167.51, 150.96, 149.84, 145.90, 140.84, 137.10, 129.89, 128.71, 124.02, 122.35, 120.23, 117.72, 112.45, 61.70, 52.05, 32.71, 28.24, 27.80, 23.68, 15.33, 15.06, Theoretical MS $C_{30}H_{42}N_2O_2$: 462.32, observed: $[M+H]^+$; 463.4.

(E)-Ethyl 3-(4-(4-(didodecylamino)styryl)pyridin-3-yl) acrylate (6b)—^{1}H NMR ($CDCl_3$): 8.68 (s, 1H), 8.47 (d, 1H, J=5.2 Hz), 8.04 (d, 1H, J=16.0 Hz), 7.45 (d, 1H, J=5.2 Hz), 7.41 (d, 2H, J=8.8 Hz), 7.14 (d, 1H, J=15.9 Hz) 7.03 (d, 1H, J=15.9 Hz), 6.62 (d, 2H, J=8.8 Hz), 6.42 (d, 1H, J=16.0 Hz), 4.29 (q, 2H, J=7.1Hz), 3.27–3.31 (m, 4H), 1.57–1.61 (m, 4H), 1.26–1.33 (m, 39H), 0.88 (t, 6H, J=7.0 Hz), ^{13}C NMR ($CDCl_3$): 166.5, 149.9, 148.9, 148.8, 144.9, 139.8, 136.0, 128.8, 127.7, 123.0, 121.3, 119.2, 116.7, 111.4, 60.7, 51.0, 31.9, 29.6, 29.6, 29.5, 29.3, 27.2, 27.1, 22.7, 14.3, 14.1, Theoretical $MSC_{42}H_{66}N_2O_2$: 630.51, observed: [M+H]+; 631.7.

(E)-Ethyl-3-(4-(4-(dimethylamino)styryl)pyridin-3-yl)acry-late (6c)—^{1}H NMR ($CDCl_3$): 8.69 (s, 1H), 8.48 (d, 1H), 8.05 (d, 1H), 7.44–7.47 (m, 3H), 7.17 (d, 1H) 7.07 (d, 1H), 6.71 (d, 2H), 6.43 (d, 1H), 4.29 (q, 2H), 3.02 (s, 6H), 1.35 (t, 3H) Theoretical $MSC_{20}H_{22}N_2O_2$: 322.17, observed: $[M+H]^+$; 323.1.

General Procedure for the Syntheses of 7a–7c (Scheme I)—To a solution of substituted aminostrylpyridine acrylate (**6a–6c**, 0.5 mmol) in ethanol (8 mL) and 2-propanol (8 mL) was added a solution of NaOH (1.5 mmol) in water (4 mL). In the case of **6c** only ethanol and water were used. The reaction mixture was stirred at room temperature for 2 h. At the end of the reaction the excess ethanol and 2-propanol were removed under reduced pressure. A solution of 3 N-HCl (3 mL) was added to the reaction mixture to neutralize the solution. The aqueous layer was extracted with CH_2Cl_2 (30 mL). The organic layer was combined, dried over Na_2SO_4, and filtered. Without purification, the amphiphilic compounds **7a–7c** were used for the next step. ^{1}H NMR showed the crude material in high purity (>95%).

(E)-3-(4-(4-(Dihexylamino)styryl)pyridin-3-yl)acrylic acid (7a)—^{1}H NMR (CD_3OD): 8.72 (s, 1H), 8.40 (d, 1H, J=6.1 Hz), 8.05 (d, 1H, J=6.1 Hz), 8.03 (d, 1H, J=16.1 Hz) 7.67 (d, 1H, J=15.7 Hz), 7.58 (d, 2H, J=8.9 Hz), 7.17 (d, 1H, J=15.7 Hz), 6.73 (d, 2H, J=8.9 Hz), 6.58 (d, 1H, J=16.1 Hz), 3.38 (t, 4H, J=7.8 Hz), 1.58–1.62 (m, 4H), 1.32–1.36 (m, 12H), 0.91 (t, 6H, J=6.8 Hz), Theoretical MS $C_{28}H_{38}N_2O_2$: 434.29, observed: $[M+H]^+$; 435.3.

(E)-3-(4-(4-(Didodecylamino)styryl)pyridin-3-yl)acrylic acid (7b)—^{1}H NMR (CD_3OD): 8.57 (s, 1H), 8.31 (d, 1H, J=5.4 Hz), 7.80 (d, 1H, J=16.0 Hz), 7.65 (d, 1H, J=5.4 Hz), 7.50 (d, 2H, J=8.8 Hz), 7.31 (d, 1H, J=15.7 Hz), 7.22 (d, 1H, J=15.7 Hz), 6.67 (d, 2H, J=8.8 Hz), 6.46 (d, 1H, J=16.0 Hz), 3.30–3.35 (m, 4H), 1.57–1.61 (m, 4H), 1.27–1.34 (m, 36H), 0.86–0.90 (m, 6H), Theoretical $MSC_{40}H_{62}N_2O_2$: 602.48, observed: $[M+H]^+$; 603.5.

(E)-3-(4-(4-(dimethylamino)styryl)pyridin-3-yl)acrylic acid (7c)—^{1}H NMR (CD_3OD): 9.06 (s, 1H), 8.72 (d, 1H), 8.43 (d, 1H), 8.06 (d, 1H), 7.99 (d, 2H), 7.89 (d, 2H), 7.74 (d, 2H), 7.66 (d, 1H), 6.72 (d, 1H), 3.29 (s, 6H), ^{13}C NMR (CD_3OD): 166.9, 152.9, 140.6, 140.2, 139.7, 135.2, 131.8, 130.0, 126.9, 123.0, 121.6, 120.2, 44.9, Theoretical $MSC_{18}H_{18}N_2O_2$: 294.14, observed: $[M+H]^+$; 295.0.

General Procedure for the Syntheses of 11a–11c (Scheme II)—To a suspension of compound **10a–10c** (30 mg) in CH_3CN was added 4-iodobenzylbromide (5 mg). The reaction mixture was refluxed for 12 h with gentle stirring. After monitoring formation of resin-bound pyridinium compound by mass spectroscopy, the excess solvent and reagent were removed by filtration. The resin-bound compound was combined and diluted in TFA/CH_2Cl_2 solution (1:1, 3 mL). The reaction mixture was stirred at room temperature for 2 h and was filtered. The combined solution was concentrated under reduced pressure and was subjected to HPLC to give the final compounds **11a–11c**.

4-(4-(Dihexylamino)styryl)-3-((5S,10S,15S,20S,25S,30S,E)-5,10,15,20,25,30,32-heptacarboxy-3,8,13,18,23,28-hexaoxo-4,9,14,19,24,29-hexaazadotriacont-1-enyl)-1-(4-iodoben-zyl)pyridinium (11a)—HPLC: MeOH/CH_3CN/H_2O=94/2/4 (0.1% TFA, 4 mL/min), retention time: 20 min, ^{1}H NMR (CD_3OD): 9.10 (s, 1H), 8.41 (d, 1H, J=7.0 Hz), 8.16 (d, 1H, J=7.0 Hz), 7.87 (d, 1H, J=15.7 Hz), 7.82 (d, 1H, J=15.9 Hz), 7.81 (d, 2H, J=8.4 Hz), 7.64 (d, 2H, J=9.0 Hz), 7.33 (d, 2H, J=8.4 Hz), 7.25 (d, 1H, J=15.9 Hz), 6.92

(d, 1H, J=15.7 Hz), 6.71 (d, 2H, J=9.0 Hz), 5.66 (s, 2H), 4,45–4.50 (m, 1H), 4.25–4.32 (m, 5H), 3.36–3.40 (m, 4H), 2.27–2.33 (m, 12H), 2.18–2.23 (m, 6H), 1.98–2.07 (m, 6H) 1.57–1.63 (m, 4H), 1.32–1.36 (m, 12H), 0.91 (m, 6H), Theoretical MS: 1425.50, observed: $[M]^+$; 1425.6, $[M+H]^{2+}$; 724.3.

4-(4-(Didodecylamino)styryl)-3-((5S,10S,15S,20S,25S,E)-5,10,15,20,25,27-hexacarboxy-3,8,13,18,23-pentaoxo-4,9,14,19,24-pentaazaheptacos-1-enyl)-1-(4-iodobenzyl)pyridinium (11b)—HPLC: MeOH/CH_3CN/H_2O=94/2/4 (0.1% TFA, 4 mL/min), retention time: 32 min, ^1H NMR (CD_3OD): 9.03 (s, 1H), 8.40 (d, 1H, J=6.7 Hz), 8.15 (d, 1H, J=6.7 Hz), 7.79–7.89 (m, 4H) 7.63 (d, 2H, J=8.8 Hz), 7.30 (d, 2H, J=8.4 Hz), 7.22 (d, 1H, J=15.4 Hz), 6.71 (d, 2H, J=8.8 Hz), 6.68 (d, 1H, J=14.9 Hz), 5.63 (s, 2H), 4,45–4.50 (m, 1H), 4.29–4.36 (m, 4H), 3.36–3.40 (m, 4H), 2.31–2.36 (m, 10H), 2.12–2.18 (m, 5H), 1.97–2.08 (m, 5H) 1.58–1.63 (m, 4H), 1.22–1.36 (m, 36H), 0.89 (m, 6H), Theoretical $MSC_{72}H_{103}IN_7O_{17}^+$: 1464.64, observed: $[M]^+$; 1464.8, $[M+H]^{2+}$; 732.9.

4-(4-(Dimethylamino)styryl)-3-((5S,10S,15S,20S,25S,E)-5,10,15,20,25,27-hexacarboxy-3,8,13,18,23-pentaoxo-4,9,14,19,24-pentaazaheptacos-1-enyl)-1-(4-iodobenzyl)pyridinium (11c)—HPLC: MeOH/CH_3CN/H_2O=40/30/30 (0.1% TFA, 4 mL/min), retention time: 16 min, ^1H NMR (CD_3OD): 8.91 (s, 1H), 8.51 (d, 1H, J=6.8 Hz), 8.22 (d, 1H, J=6.8 Hz), 7.95 (d, 1H, J=15.7 Hz), 7.81–7.87 (m, 3H) 7.63 (d, 2H, J=9.0 Hz), 7.28 (d, 2H, J=8.4 Hz), 7.22 (d, 1H, J=15.9 Hz), 6.75–6.79 (m, 3H), 5.62 (s, 2H), 4,45–4.50 (m, 1H), 4.40–4.44 (m, 4H), 3.36 (s, 6H), 2.31–2.40 (m, 10H), 2.15–2.25 (m, 5H), 1.98–2.08 (m, 5H),Theoretical MS $C_{50}H_{59}IN_7O_{17}^+$: 1156.30, observed: $[M]^+$; 1156.4 $[M+H]^{2+}$; 578.6.

Radiosynthesis of [^{125}I]15a and [^{125}I]15c (Scheme III)—To a solution of compound **14a** (6 mg) suspended in 300 μL in MeOH was added 300 μL of NCS solution (0.8 mg in 1 mL of MeOH). To this was added a solution of [^{125}I]NaI (2.78 mCi, MP Biomedicals, Costa Mesa, CA) diluted with 15 μL of phosphate buffered saline. After 60 min at room temperature, the excess methanol was removed with the resin in the vial. The radioactivity of the remained resin was 2.38 mCi while the methanol solution was 300 μCi. To the reaction vial was added 200 μL of anhydrous dichloromethane and 200 μL of TFA. The reaction mixture was stirred very slowly at room temperature for 90 min. The dichloromethane and TFA were removed under a gentle stream of nitrogen. The reaction mixture was diluted with 500 μL of MeOH/H_2O (80/20, 0.5% TEA). HPLC conditions for **15a** and **15c** were 38% MeOH/62% H_2O/0.3% TEA and 15% MeOH/85% H_2O/ 0.3% TEA with a flow rate of 1.5 mL/min on a Waters Radial Pak analytical column (8×10 mm). About 1.2 mCi of **15a** and **15c** (retention time: 11.5 and 7.2 min) were collected and evaporated to dryness under vacuum (43% RCY, 1500 mCi/ μmol). They were formulated in 250 μL saline for subsequent imaging.

Biology

PSMA Substrate Specificity—Glutamate release from the synthesized conjugates was determined using a fluorescence-based assay. Lysates of LNCaP cell extracts were incubated with the substrates at different concentrations. ASP-polyglutamate conjugates and NAAG were incubated with PSMA-expressing LNCaP cell extracts in 0.1 M Tris-HCl (pH

7.5) at 37 °C for 2 h. The amount of glutamate released by the hydrolysis of C-terminal glutamates was measured by incubating with a working solution of the Amplex Red glutamic acid kit (Molecular Probes Inc., Eugene, OR, USA). The fluorescence was measured with a VICTOR^{3}V multilabel plate reader (Perkin Elmer Inc., Waltham, MA, USA) with excitation at 530 nm and emission at 560 nm.

Cell Lines and Mouse Models—PC3 PIP (PSMA$^+$) and PC3 flu (PSMA$^-$) cell lines were obtained from Dr. Warren Heston (Cleveland Clinic, USA) and were maintained as previously described. All cells were grown to 80%–90% confluence before trypsinization and formulation in Hank's Balanced Salt Solution (HBSS, Sigma, St. Louis, MO) for implantation into mice. All animal studies were undertaken in full compliance with institutional guidelines related to the conduct of animal experiments. Male severe combined immunodeficient (SCID) mice (Charles River Laboratories, Wilmington, MA) were implanted subcutaneously with 1–5 ×10^6 cells forward of each flank. PSMA$^+$ PC3 PIP cells were implanted behind the left flankand PSMA$^-$ PC3 flu cells were implanted behind the right flank. Mice were imaged or used in biodistribution assays when the tumor xenografts reached 3–5 mm in diameter.

Single Photon Emission Computed Tomography-Computed Tomography (SPECT-CT) Imaging of [^{125}I]15a and [^{125}I]15c—A single SCID mouse implanted with both a PSMA+PC3 PIP and a PSMA-PC3 flu xenograft was injected intravenously with ~700 μCi (25.9 MBq) of [^{125}I]**15a–15c** in saline. The mouse was positioned on the X-SPECT (Gamma Medica, Northridge, CA) gantry and was scanned using two low energy, high-resolution pinhole collimators (Gamma Medica) rotating through 360° in 6° increments for 45 s per increment. Images were reconstructed using LumaGEM software (Gamma Medica, Northridge, CA). Immediately following SPECT acquisition the mice were then scanned by CT (X-SPECT) over a 4.6 cm field-of-view using a 600 A, 50 kV beam. The SPECT and CT data were then coregistered using the supplier's software (Gamma Medica) and displayed using AMIDE (http://amide.sourceforge.net/). Data were reconstructed using the ordered subsets-expectation maximization (OS-EM) algorithm.

Biodistribution of [^{125}I]15a and 15c—Blood was collected immediately after sacrifice by cardiac puncture and heart, lung, liver, stomach, pancreas, spleen, white fat, kidney, muscle, small intestine, large intestine, urinary bladder, and tumor xenografts were harvested, weighed, and counted in an automated gamma counter (LKB Wallace 1282 Compugamma CS Universal Gamma Counter). Animals were sacrificed at 24 and 144 h postinjection for **15c** and **15a**, respectively. Tissue radiopharmaceutical uptake values were calculated as percent injected dose per gram (% ID/g).

HPLC of Tumor Cell Extracts—Compound **11c** in LNCaP cell extracts (50 μM in 100 μL) was incubated at 37 °C for 30 min, 3 h, and 20 h. The mixture was diluted with HPLC solvent system (MeOH/CH_3CN/H_2O=40/30/30, 0.1% TFA, 300 μL) and the crude solution (50 μL) was subjected to was subjected to the analytical HPLC system. The peaks were monitored at 254 nm and confirmed by mass spectrometer.

Molecular Modeling—Molecular modeling studies of **11c** were performed with Discovery Studio 2.1 (Accelrys Inc. San Diego, USA) implemented on a Windows XP2 system. The PSMA crystal structure (PDB ID: 2C6C) was downloaded from the Protein Data Bank. The 3-D structure of **11c** was superimposed upon GPI-18431 by tethering four attachment points (N-CH(COO-)-CH_2 in glutamate). The coordinates of superimposed **11c** were transferred into the apoprotein of 2C6C and merged in the system. The 2C6C/**11c** complex system was minimized by modifying default settings (max steps: 20000, max RMS gradient: 0.01, implicit solvent model: Generalized Born with a simple switching (GBSW), dielectric constant: 1, implicit solvent dielectric constant: 80). Consecutive simulations of the obtained complex system from minimization were carried out using a standard simulation cascade protocol, which performs several consecutive simulations (minimization, heating, equilibration, production) for a 2C6C/**11c** complex system. For 2C6C/**11c** dynamics with constraints, amino acid residues within 7 Å of **11c** remained flexible while all other amino acids were fixed. Dynamics simulation was performed by slightly modifying default settings [minimization algorithm: steepest descent (max steps: 500, minimization RMS gradient: 0.1), minimization algorithm2: conjugate gradient (max steps: 500, RMS gradient: 0.0001, heating (steps: 2000, initial temperature: 50.0, target temperature: 300.0), equilibration (steps: 1000, target temperature: 300.0), implicit solvent model: GBSW, dielectric constant: 1, solvent dielectric constant: 80)].

Results and Discussion

Chemistry

The synthetic routes for γ- and α-linked ASP-pentaglutamates or ASP-hexaglutamates are outlined in Schemes I and II. Key intermediate aminostrylpyridines **7a–7c** were prepared in four steps from 4-(dialkylamino) benzaldehydes **3a–3c** which were synthesized by reacting *N*,*N*-dialkylaniline **2a–2c** with $POCl_3$ in DMF.[32,33] Lithiation of 3-bromo-4-methylpyridine using lithium diisopropylamide (LDA) and subsequent addition of **3a–3c** gave a racemic mixture of the *erythro* and *threo* forms of carbinols **4a–4c** in 59%–66% yield. Dehydration of **4a–4c** under acidic condition afforded strylpyridines **5a–5c** in 83%–88% yield with the *E*-isomer as the major product. Palladium-catalyzed Heck coupling of **5a–5c** with ethylacrylate in DMF at 130 °C using palladium acetate and triphenylphosphine gave aminostryl-pyridine acrylates **6a–6c** in 60%–68% yield. The less lipophilic dimethyl analog **7a** was obtained by reacting **6a** with NaOH in a mixture of ethanol/water (2:1). However, hydrolysis of the more lipophilic dihexyl analog **6b** and didodecyl analog **6c** occurred by treating NaOH in a mixture of 2-propanol/EtOH/water (2:2:1). 2-Propanol improved the solubility of the lipophilic ethylesters **6b–6c**.

The other key polyglutamate intermediates, poly-γ-glutamate **9** and poly-α-glutamate **12** were prepared by utilizing solid phase chemistry. Reaction of the Fmoc-Glu(OtBu)-preloaded Wang resin with 20% piperidine in DMF for 60 min, followed by coupling with Fmoc-Glu-OtBu under peptide coupling conditions (HBTU, HOBt, DIPEA, DMF, 2 h) gave Fmoc-Glu(OtBu)-Glu(OtBu)-resin. ubsequent deprotection of the Fmoc group and coupling with Fmoc-Glu-OtBu in 3 or 4 consecutive reactions afforded compounds **9a** and **9b**,

respectively. To prepare resin-bound α-linked penta-glutamate **12**, Fmoc-Glu(OtBu)-OH was used instead of Fmoc-Glu-OtBu in each reaction cycling step.

Conjugations of **7a–7c** with **9a–9b** under peptide coupling conditions (TBTU, HOBt, and DIPEA) gave compounds **10a–10c**. Reaction of **10a–10c** with 4-iodobenzyl bromide in acetonitrile under reflux for 12 h, followed by deprotection of the *tert*-butyl (*t*Bu) groups and removal of Wang resin by treating trifluoroacetic acid (TFA), afforded the γ-linked ASP-glutamates **11a–11c**. The α-linked ASP-glutamate conjugates **13a–13c** were prepared in the same synthetic strategy as that for **11a–11c**. The syntheses of ^{125}I-labeled, γ-linked ASP-glutamates **15a–15c** for *in vivo* imaging studies are shown in Scheme III. Reaction of **10a–10c** with 4-(tributylstannyl)benzyl bromide, which was obtained from 4-bromobenzyl alcohol in 3 steps, gave the radioiodination precursors **14a–14c**. Radioiodination-destannylation of **14a–14c** with Na[^{125}I]I and *N*-chlorosuccinimide (NCS), followed by removal of *t*Bu groups and Wang resin with TFA in dichloromethane, afforded the [^{125}I]I-labeled γ-linked ASP-glutamate conjugates **15a–15c**. The radiochemical purity of each compound was > 97%, with minimum specific activity >42.5 GBq/μmol.

Biology

In order to investigate the ability of the synthesized compounds to serve as substrates for PSMA, we determined the release of glutamate from ASP-polyglutamate conjugates by incubating them with PSMA-expressing LNCaP cell extracts (Figure 2). The fluorescence intensity of γ-linked ASP-pentaglutamate conjugates **11b** and **11c** increased in a concentration-dependent manner while compounds **13a** (not shown) and **13b**, the α-linked ASP-pentaglutamate conjugates, demonstrated background levels of fluorescence at the same concentrations. Incubation with NAAG provided a pattern similar to that produced by the γ-linked ASP-glutamate conjugates. These data indicate that γ-linked ASP-penta-glutamate conjugates are substrates for PSMA while the α-linked ASP-pentaglutamate conjugates are not.

We attempted imaging of ^{125}I-labeled **15a–15c** in SCID mice harboring experimental models of PCa. Isogenic PSMA$^+$ PIP and PSMA$^-$ flu tumors were grown in opposite flanks, and animals were imaged with SPECT-CT (Figure 3). Imaging showed that lipophilic conjugates **15a** and **15b** had extended blood pool residence times and significant accumulation in the liver. However, selective uptake within PSMA$^+$ PIP tumors over PSMA$^-$ flu tumors was not observed. Preliminary biodistribution studies of **15a** showed 3.14%ID/g for PIP and 3.02%ID/g for flu tumors at 6 days post-injection (Table I).

To investigate further the nonspecific uptake of **15a−15c** in the PSMA-expressing tumors, the cleavage of the polyglutamate moiety of the γ-linked ASP conjugates was studied. HPLC studies of **11c** (50 μM) in LNCaP cell extracts (100 μL) exhibited slow cleavage of the C-terminal glutamate (24 h), indicating that the designed substrates are recognized by but only very slowly cleaved by PSMA (Figure 4). Computational docking studies of **11c** with the crystal structure of PSMA were undertaken to elucidate how **11c** binds to the active site of PSMA and why glutamate liberation is not as effective as for poly-γ-glutamyl folate. As shown in Figure 5, the ASP moiety is almost perpendicular to the pentaglutamate moiety,

suggesting that the bulky ASP region of the T-shape **11c** appears to prevent the C-terminus glutamate moiety from gaining access to the enzymatic catalytic regions (Glu 424 and zinc ions) of PSMA. Quite possibly that T-shape pattern prevents the cleaved product of **11c** from binding to the active site more productively than **11c** itself.

Conclusions

We designed, synthesized, and evaluated substrate-based PSMA-targeting imaging agents for *in vivo* animal studies. We successfully introduced ^{125}I into the ASP-dyes using solid-phase chemistry and confirmed that γ-linked ASP conjugates are better PSMA substrates as compared to the corresponding α-linked ASP conjugates. Although *in vivo* SPECT-CT imaging of the designed ASP-polyglutamate conjugates (**15a** and **15c**) did not show selective uptake in PSMA-positive over PSMA-negative tumors, the more lipophilic **15c** circulated in the body for up to six days and accumulated in the tumor higher than 3%ID/g. *In vitro* HPLC studies and molecular modeling with **11 c** exhibited the limitation of ASP-conjugates with a T-shape, indicating that a comprehensive structural modification of the current PSMA-based substrates will be needed to identify better substrates of PSMA to achieve the successful substrate-based imaging agents for this target.

Acknowledgments

The authors are grateful for financial support from National Institutes of Health Grants MH080580 and CA134675.

References

1. Zhou J, Neale JH, Pomper MG, Kozikowski AP. Nat Rev Drug Discov. 2005; 4:1015. [PubMed: 16341066]
2. Serda RE, Adolphi NL, Bisoffi M, Sillerud LO. Mol Imaging. 2007; 6:277. [PubMed: 17711783]
3. Banerjee SR, Foss CA, Castanares M, Mease RC, Byun Y, Fox JJ, Hilton J, Lupold SE, Kozikowski AP, Pomper MG. J Med Chem. 2008; 51:4504. [PubMed: 18637669]
4. Chen Y, Foss CA, Byun Y, Nimmagadda S, Pullambahatla M, Fox JJ, Castanares M, Lupold SE, Babich JW, Mease RC, Pomper MG. J Med Chem. 2008; 51:7933. [PubMed: 19053825]
5. Chen Y, Dhara S, Banerjee SR, Byun Y, Pullambhatla M, Mease RC, Pomper MG. Biochem Biophys Res Commun. 2009; 390:624. [PubMed: 19818734]
6. Banerjee SR, Pullambhatla M, Byun Y, Nimmagadda S, Green G, Fox JJ, Horti A, Mease RC, Pomper MG. J Med Chem. 2010; 53:5333. [PubMed: 20568777]
7. Banerjee SR, Pullambhatla M, Byun Y, Nimmagadda S, Foss CA, Green G, Fox JJ, Lupold SE, Mease RC, Pomper MG. Angew Chem Int Ed. 2011; 50:9167.
8. Zhang W, Slusher B, Murakawa Y, Wozniak KM, Tsukamoto T, Jackson PF, Sima AAF. J Neurol Sci. 2002; 194:21. [PubMed: 11809162]
9. Tiffany CW, Cai NS, Rojas C, Slusher BS. Eur J Pharm. 2001; 427:91.
10. Ghadge GD, Slusher BS, Bodner A, Dal Canto M, Wozniak K, Thomas AG, Rojas C, Tsukamoto T, Majer P, Miller RJ, Monti AL, Roos RP. Proc Natl Acad Sci USA. 2003; 100:9554. [PubMed: 12876198]
11. Guilarte TR, Hammoud DA, McGlothan JL, Caffo BS, Foss CA, Kozikowski AP, Pomper MG. Schizophr Res. 2008; 99:324. [PubMed: 18191545]
12. Sacha P, Zamecnik J, Bacrinka C, Hlouchova K, Vicha A, Mlcochova P, Hilgert I, Eckschlager T, Konvalinka J. J Neurosci. 2007; 144:1361.
13. Duthie SJ, Narayanan S, Brand GM, Pirie L, Grant G. J Nutr. 2002; 132:2444s. [PubMed: 12163709]

14. Chang SS, Reuter VE, Heston WDW, Bander NH, Grauer LS, Gaudin PB. Cancer Res. 1999; 59:3192. [PubMed: 10397265]
15. Tsukamoto T, Wozniak KM, Slusher BS. Drug Discov Today. 2007; 12:767. [PubMed: 17826690]
16. Davis MI, Bennett MJ, Thomas LM, Bjorkman PJ. Proc Natl Acad Sci USA. 2005; 102:5981. [PubMed: 15837926]
17. Mesters JR, Barinka C, Li WX, Tsukamoto T, Majer P, Slusher BS, Konvalinka J, Hilgenfeld R. EMBO J. 2006; 25:1375. [PubMed: 16467855]
18. Plechanovova A, Byun Y, Alquicer G, Skultetyova L, Mlcochova P, Nemcova A, Kim HJ, Navratil M, Mease R, Lubkowski J, Pomper MG, Konvalinka J, Rulisek L, Barinka C. J Med Chem. 2011; 54:7535. [PubMed: 21923190]
19. Wang HF, Byun Y, Barinka C, Pullambhatla M, Bhang HEC, Fox JJ, Lubkowski J, Mease RC, Pomper MG. Bioorg Med Chem Lett. 2010; 20:392. [PubMed: 19897367]
20. Barinka C, Byun Y, Dusich CL, Banerjee SR, Chen Y, Castanares M, Kozikowski AP, Mease RC, Pomper MG, Lubkowski J. J Med Chem. 2008; 51:7737. [PubMed: 19053759]
21. Zhang AX, Murelli RP, Barinka C, Michel J, Cocleaza A, Jorgensen WL, Lubkowski J, Spiegel DA. J Am Chem Soc. 2010; 132:12711. [PubMed: 20726553]
22. Liu TC, Wu LY, Kazak M, Berkman CE. Prostate. 2008; 68:955. [PubMed: 18361407]
23. Liu H, Rajasekaran AK, Moy P, Xia Y, Kim S, Navarro V, Rahmati R, Bander NH. Cancer Res. 1998; 58:4055. [PubMed: 9751609]
24. Johnson M, Karanikolas BDW, Priceman SJ, Powell R, Black ME, Wu HM, Czernin J, Huang SC, Wu L. J Nucl Med. 2009; 50:757. [PubMed: 19372484]
25. Fu DX, Tanhehco YC, Chen JM, Foss CA, Fox JJ, Lemas V, Chong JM, Ambinder RF, Pomper MG. Clin Cancer Res. 2007; 13:1453. [PubMed: 17332288]
26. Zhang ZX, Liu YY, Jhiang SM. J Clin Endocrinol Metab. 2005; 90:6131. [PubMed: 16105966]
27. Mhaka A, Gady AM, Rosen DM, Lo KM, Gillies SD, Denmeade SR. Cancer Biol Ther. 2004; 3:551. [PubMed: 15044850]
28. Anderson MO, Wu LY, Santiago NM, Moser JM, Rowley JA, Bolstad ES, Berkman CE. Bioorg Med Chem. 2007; 15:6678. [PubMed: 17764959]
29. Lambert C, Mease RC, Avren L, Le T, Sabet H, McAfee JG. Nucl Med Biol. 1996; 23:417. [PubMed: 8832696]
30. Albright JW, Mease RC, Lambert C, Albright JF. Mech Ageing Dev. 1998; 101:197. [PubMed: 9622224]
31. Mease RC, Lambert C, McAfee JG. J Nucl Med. 1999; 40:318.
32. Raimundo JM, Blanchard P, Gallego-Planas N, Mercier N, Ledoux-Rak I, Hierle R, Roncali J. J Org Chem. 2002; 67:205. [PubMed: 11777461]
33. Ozturk T, Klymchenko AS, Capan A, Oncul S, Cikrikci S, Taskiran S, Tasan B, Kaynak FB, Ozbey S, Demchenko AP. Tetrahedron. 2007; 63:10290.

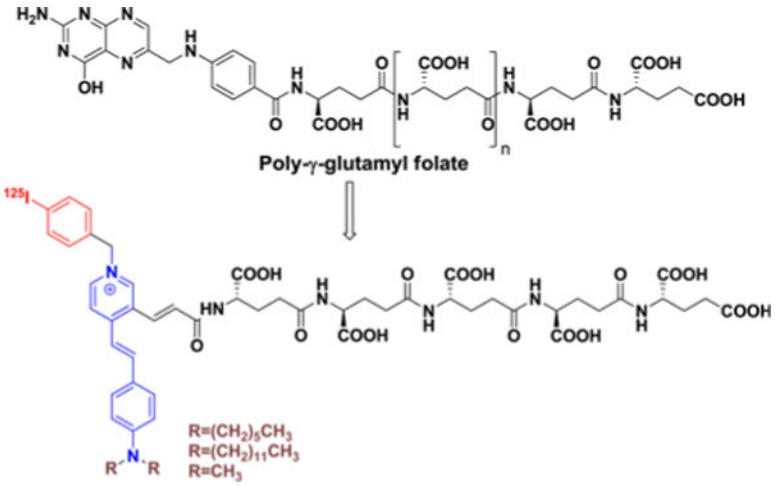

Figure 1.
Design of aminostrylpyridium (ASP)-polyglutamate conjugates.

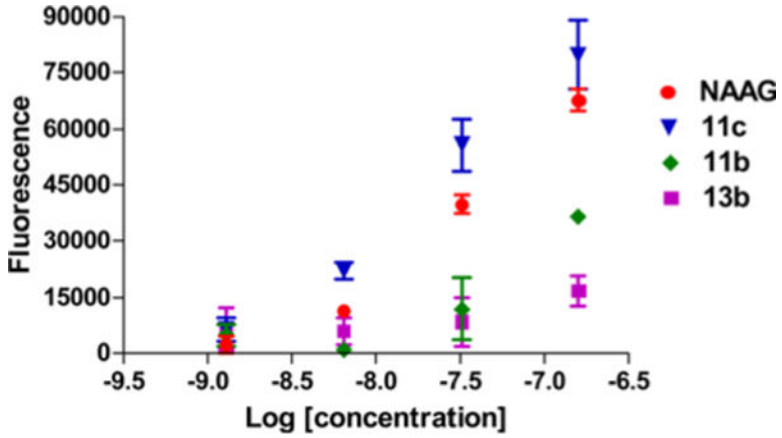

Figure 2.
Glutamate production of **11b, 11c, 13b**, and NAAG.

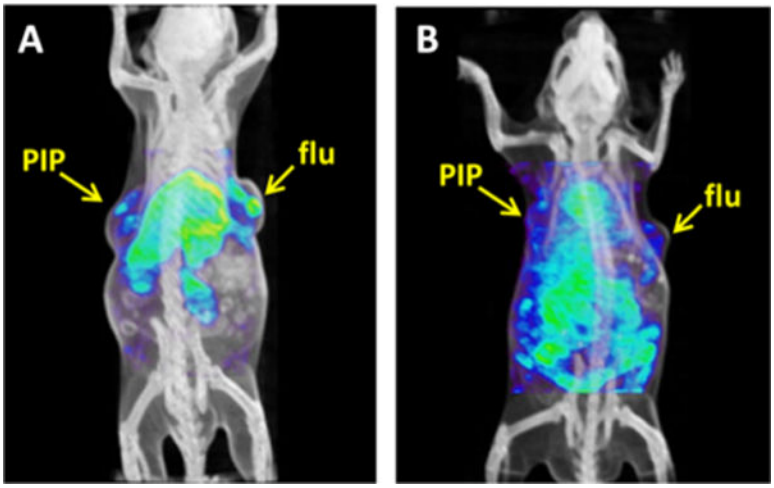

Figure 3.

SPECT-CT images of **15a** at 6 days (A) and of **15c** at 24 h post-injection (B). PIP=$PSMA^{+}$ PC3 tumors; flu=$PSMA^{-}$ PC3 tumors.

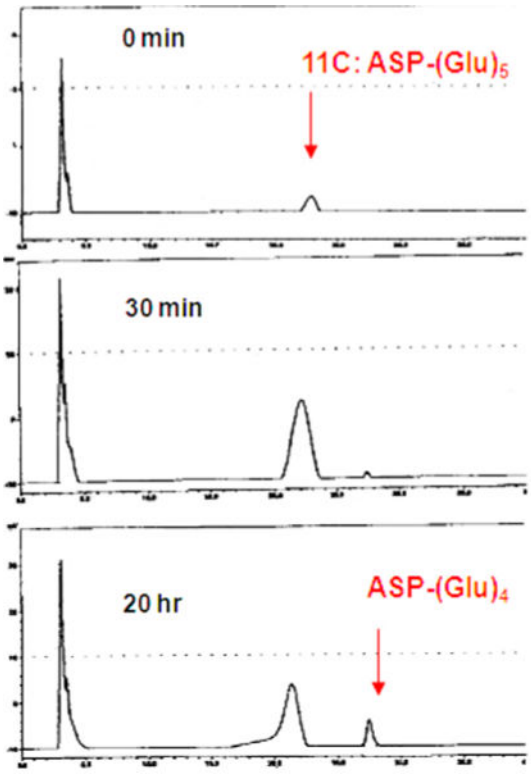

Figure 4.
HPLC trace of **11c**.

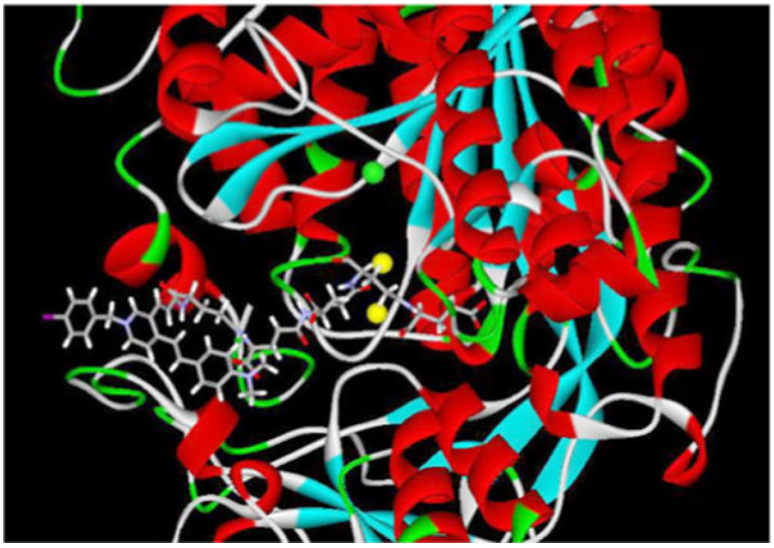

Figure 5.
Binding mode of **11c** in the active site of PSMA.

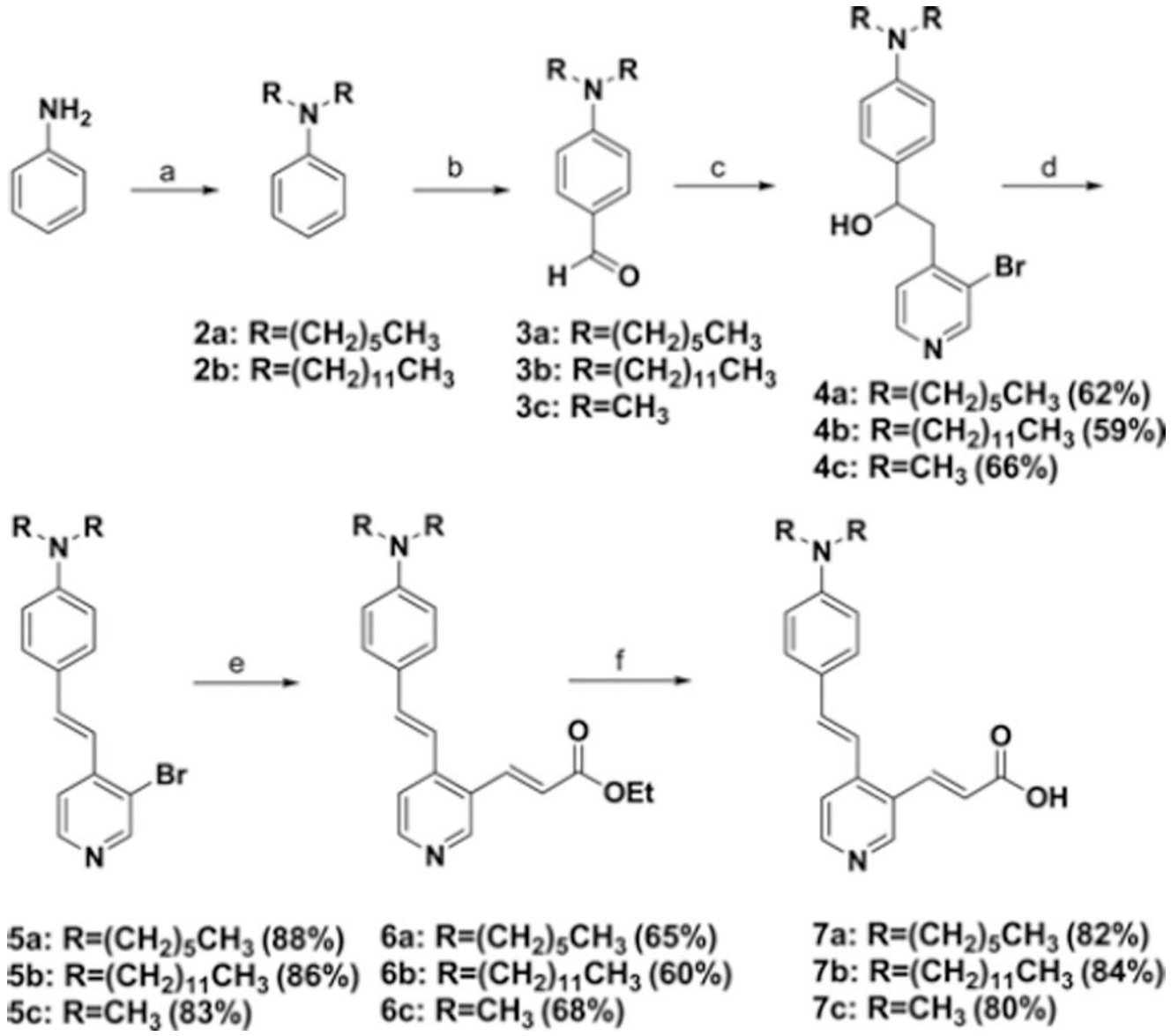

Scheme I.

Synthetic route to aminostrylpyridine moieties. Reagents and conditions: (a) K_2CO_3, DMF, 1-iodohexane (**2a**) or 1-iodo-dodecane (**2b**), (b) $POCl_3$, DMF, (c) 3-bromo-4-methylpyridine, LDA, Et_2O, (d) 3N-HCl, dioxane, 60 °C, (e) ethylacrylate, PPh_3, $Pd(OAc)_2$, TEA, DMF, 130 °C, (f) NaOH, H_2O/EtOH/*i*-PrOH.

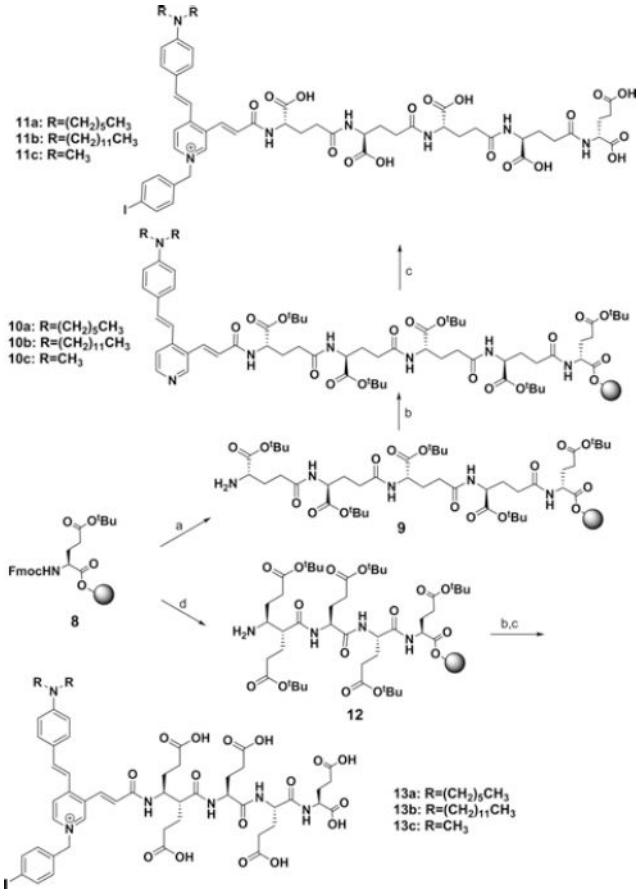

Scheme II.

Synthetic route for resin-bound polyglutamates. Reagents and conditions: (a) i: 20% piperidine in DMF, rt, 60 min, ii: Fmoc-Glu-OtBu, HATU, HOBt, DIPEA, DMF, (b) HATU, HOBt, DIPEA, DMF, **7a** (for **10a**), **7b** (for **10b**), or **7c** (for **10c**), (c) i: 4-iodobenzyl chloride, CH_3CN, ii: TFA/CH_2Cl_2, (d) 20% piperidine in DMF, rt, 60 min, ii: Fmoc-Glu(OtBu)-OH, HATU, HOBt, DIPEA, DMF.

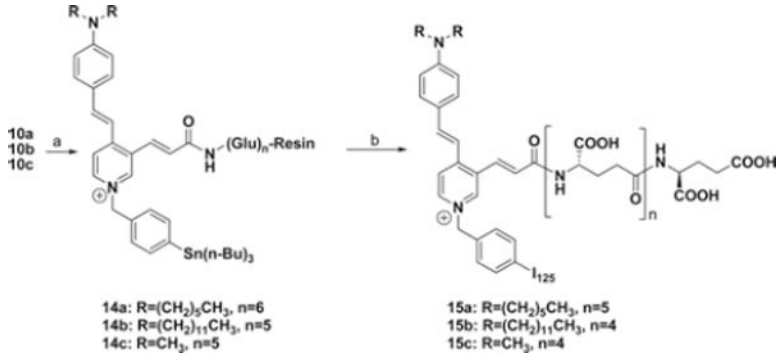

Scheme III.

Synthetic route to [^{125}I]**15a** and [^{125}I]**15c**. Reagents and conditions: (a) i: 4-((bromomethyl)phenyl)tributylstannane, CH_3CN, reflux, 24 h, (b) i: Na[^{125}I]I, *N*-chlorosuccinimide, methanol (0.1% acetic acid), rt, 2 h, ii: TFA/CH_2Cl_2 (1:1), rt, 90 min.

Table I

Ex vivo Biodistribution Studies of 15a at 6 Days and 15c at 24 h Post-Injection

Organ	15a	15c
Blood	0.35	0.31
Heart	2.06	0.12
Lung	3.01	0.30
Liver	15.15	0.49
Stomach	1.33	0.07
Pancreas	0.66	0.06
Spleen	23.79	0.32
Kidney	6.02	0.50
Muscle	0.52	0.04
Small Intestine	2.13	0.06
Large Intestine	2.98	0.07
Bladder	2.35	0.14
PIP-Tumor	3.14	0.15
Flu-Tumor	3.02	0.12